

Fabrication of a SOI Based Channel-shifted Multimode Interference Coupler *

Wang Zhangtao, Fan Zhongchao, Chen Shaowu, Yu Jinzhong

State Key Laboratory on Integrated Optoelectronics, Institute of Semiconductors, the Chinese Academy of Sciences, Beijing 100083

Abstract A silicon-on-insulator based channel-shifted multimode interference coupler is designed and fabricated. A two dimensional beam propagation method is used to analyze the dependence of coupler's performances on the width and length of the multimode waveguide. The device fabricated has a power shift ratio of 73 and an excess loss of about 2.2 dB. An enhancement of fabrication accuracies could further improve the coupler performances.

Keywords SOI; Multimode interference; Channel-shifted
CLCN TN252 Document Code A

0 Introduction

Channel-shifted components are indispensable elements in many applications of integrated optics. They have been widely used to shift light inside single device or among various devices on a single substrate^[1]. An intersecting waveguide made of two S-shaped bent waveguides is one of important channel-shifted devices. However, this configuration requires a big intersecting angle to avoid the angle dependent coupling of the two intersecting modes and also because of the finite lithographic resolution^[2]. Consequently, to obtain a big intersecting angle, the device should expand its size in both longitudinal and lateral direction, which will limit its application in integrated circuits.

Multimode interference (MMI) optical devices have some excellent characteristics such as compactness, relaxed fabrication tolerance, polarization insensitivity and large optical bandwidth^[3]. MMI-based couplers have been realized in various substrate such as SiO₂, InP and GaAs. However, these devices are mainly used as 3 dB splitters or combiners. For these reasons, we have designed and fabricated channel-shifted MMI couplers in silicon-on-insulator (SOI) technology. The devices have simple structure and compact size.

1 Structure

The schematic diagram of the channel-shifted MMI coupler is shown in Fig. 1. The device consists of two

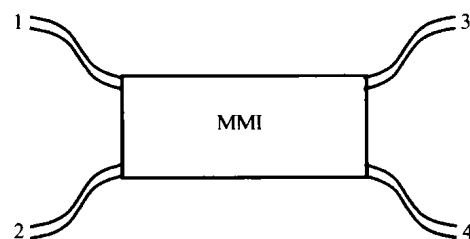


Fig. 1 Schematic diagram of channel-shifted MMI coupler single-mode input waveguides, a planar multimode waveguide and two single-mode output waveguides. The MMI coupler fulfills the conditions for general interference. Based on the self-imaging effect, the coupler can shift the light from port 1 to port 4 or from port 2 to port 3. The length of the multimode waveguide can be expressed as^[4]

$$L = 3L_{\pi} = \frac{4n_r W_{\text{eff}}^2}{\lambda} \quad (1)$$

where n_r is the refractive index of the multimode section, W_{eff} is the effective width of the multimode waveguide, λ is the free space wavelength of the light. Access waveguides in the coupler are based on a multi-micron, large cross-section rib structure fabricated on SOI materials^[5], as shown in Fig. 2.

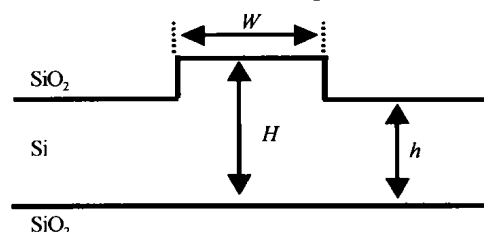


Fig. 2 Schematic graph of SOI rib waveguide

2 Design and fabrication

In our design, the free space wavelength is 1.55 μm , the width of single-mode access waveguides and multimode waveguide are 4 and 20 μm , respectively. The multimode waveguide is of 4853 μm long, predicted by effective index method and two-dimensional beam propagation method (2-D BPM). The etching depth of the SOI rib waveguides is 1.75 μm . S-bends have

*Project supported by National Natural Science Foundation of China (No. 69990540), National 863 Project (No. 2002AA312060) and State Key Development Program for Basic Research of China (No. G20000366)

Tel: 010-82304076 Email: raul_wzt@163.com

Received date: 2003-09-08

been used to space access waveguides far enough apart to minimize optical interaction. The radius of S-bends is 30 mm to assure low curvature losses. When the S-bends are introduced, the device dimensions are $36 \times 6853 \mu\text{m}^2$. By using the 2-D BPM, the optical intensity distribution inside the channel-shifted coupler is obtained and shown in Fig. 3.

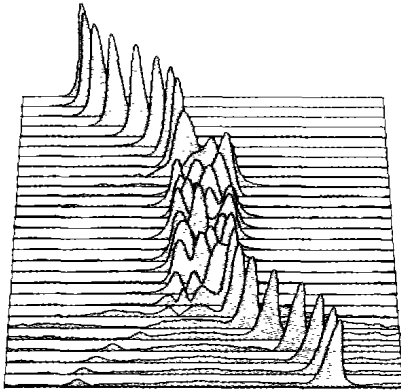


Fig. 3 Simulated optical intensity distribution inside channel-shifted coupler

BESOI wafer with a $1 \mu\text{m}$ thick insulating silicon dioxide layer and a $5 \mu\text{m}$ top single crystal silicon layer is chosen for our investigations. A Cr layer of $0.15 \mu\text{m}$ thickness was sputtered on the wafer as the etching mask. Then patterns were defined with a lithography process, followed by inductively coupled plasma (ICP) etching with the $\text{C}_4\text{F}_8/\text{SF}_6/\text{O}_2$ mixture gases. After the etching, a layer of $0.4 \mu\text{m}$ SiO_2 was deposited on the wafer by plasma enhanced chemical vapor deposition (PECVD) to avoid ruining the core region. In order to compensate the lateral corrosion during the ICP etching process, the width of the MMI section was respectively $0.2, 0.4, 0.6, 0.8 \mu\text{m}$ wider than the design value (i. e. $20 \mu\text{m}$). Fig. 4 shows the SEM graph of the cross-section of two output waveguides in the coupler.

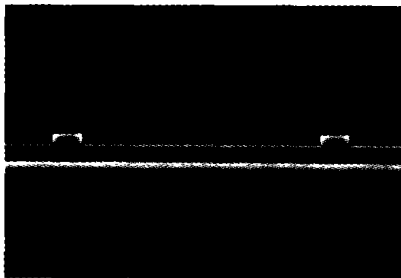


Fig. 4 SEM graph of the cross-section of two output waveguides in the coupler

3 Results and discussion

The light from the fiber at wavelength $\lambda = 1.55 \mu\text{m}$ was coupled into the rib waveguides through the cleaved endface of an input waveguide, and then the light propagated from the waveguide was collected by a $20 \times$ microscope objective, which is then fed either

into a CCD camera or a power meter as required. To evaluate the performance of the channel-shifted coupler, power shifting ratio (PSR) and excess loss (EL) are defined as

$$PSR = \frac{P_1}{P_2} \quad (1)$$

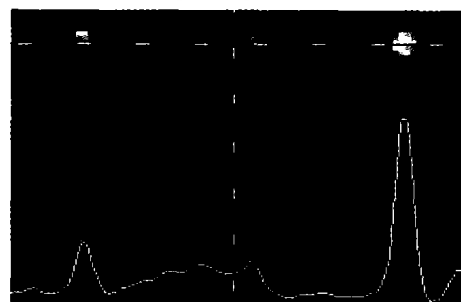
$$EL = 10 \log \left(\frac{P_1 + P_2}{P_0} \right) \quad (2)$$

where P_1 and P_2 ($P_1 > P_2$) are the output powers in the two output ports, respectively. P_0 is the output power from the straight single-mode waveguide under the same testing environments.

The near-field images in two output ports are shown in Fig. 5. The results show that the coupler can realize the functions of channel-shifting. However, some crosstalk emerged in the unwanted ports in both channels. The PSR of paths from port 1 to port 4 and from port 2 to port 3 are 73 and 66, respectively. The measured excess loss is about 2.2 dB. The big index difference and the cross-section mismatch between the waveguide and fiber core, as well as the sidewall roughness of SOI waveguide caused by ICP etching contribute to these losses. Polishing the output waveguide facets and depositing an antireflection coating layer on the facets could reduce the excess loss.



(a) port 1 → port 4



(b) port 2 → port 3

Fig. 5 Measured near-field images in two output ports

For a channel-shifted coupler, it's the design of multimode waveguide that determine its performance. During the ICP etching process, uncertainty of lateral corrosion bring about the width deviation of multimode waveguide, which results in the deviation of multimode waveguide length from the design value. These errors surely deteriorate the performance of the coupler,

which characterized by the decrease of *PSR* and increase of excess loss. By using the 2-D BPM, the dependence of *PSR* and excess loss on the width and length of multimode waveguide is simulated, as shown in Fig. 6. The results indicate that the coupler has promising *PSR* and excess loss only within a certain range on width and length of multimode section. We predict that, by further optimization of the design and enhancement of dry etching controllability, the coupler's performance could be drastically improved.

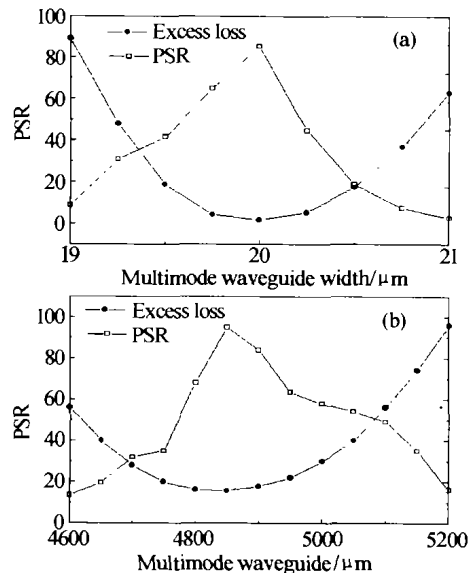


Fig. 6 Dependence of *PSR* and excess loss on (a) multimode waveguide width, (b) multimode waveguide length

4 Conclusion

In conclusion, we have successfully designed and fabricated channel-shifted couplers in SOI technology. Rib waveguides were formed by our ICP dry etching with the $\text{C}_4\text{F}_8/\text{SF}_6/\text{O}_2$ mixture gases. 2-D BPM has been used to analyze the factors which will affect the coupler's performances. The device fabricated has a *PSR* of 73 and an excess loss of about 2.2 dB. Enhancement of fabrication accuracies could further improve the coupler performance.

References

- 1 Papadimitriou G I, Papazoglou C, Pomportsis A S. Optical switching: switch fabrics, techniques, and architectures. *J Lightwave Technol*, 2003, **21**(2): 384 ~ 397
- 2 Aretz K, Bulow H. Reduction of crosstalk and losses of intersecting waveguide. *Electron Lett*, 1989, **25**(11): 730 ~ 731
- 3 Soldano L B, Pennings E C M. Optical multi-mode interference devices based on self-imaging: Principles and applications. *J Lightwave Technol*, 1995, **13**(4): 615 ~ 627
- 4 Bachmann M, Besse P, Melchior H. General self-imaging properties in $N \times N$ multimode interference couplers including phase relations. *Appl Opt*, 1994, **33**(18): 3905 ~ 3911
- 5 Soref R A, Schmidtchen J, Petermann K. Large single-mode rib waveguides in GeSi/Si and Si-on-SiO₂. *IEEE J Quant Electron*, 1991, **27**(8): 1971 ~ 1973

SOI 通道转换型多模干涉耦合器的研究

王章涛 樊中朝 陈少武 余金中

(中国科学院半导体研究所, 集成光电子国家重点联合实验室, 北京 100083)

收稿日期: 2003-09-08

摘要 设计和制作了基于 SOI 的通道转换型多模干涉耦合器。用二维 BPM 方法分析了耦合器的性能与多模波导宽度和长度的依赖关系。制作出的耦合器能实现良好的通道转换, 器件的功率转换比为 73, 附加损耗为 2.2 dB。提高器件制作的精度将能进一步改善耦合器的性能。

关键词 SOI; 多模干涉; 通道转换



Wang Zhangtao received master degree in material science and engineering from Northeastern University in March, 2001. At the present, he is a doctor at the Institute of Semiconductors, the Chinese Academy of Sciences. His current research interests are involved in Silicon-based integrated optoelectronics.